ON THE REPRESENTATION OF SNOW IN BULK MICROPHYSICAL PARAMETERIZATIONS

Mark T. Stoelinga,
Christopher P. Woods, John D. Locatelli, and Peter V. Hobbs

University of Washington, Seattle, WA

Why work with a "classic" single-moment 5-class bulk scheme?

[specifically, the Reisner et al. (1998) / Thompson et al. (2004), or "R-T" scheme]:

Sophistication of Grid-resolved Microphysics

Low ⟵⟶ **High**

Intentionally simple schemes (oper. NWP)	"Classic" SM 5-class bulk schemes	More classes/ More moments/ Gamma dist.	Spectrally explicit "bin" schemes

As computer power increases, enhanced sophistication in cloud microphysics will always compete with the desire to:

- **Increase resolution**
- **Enhance other physics schemes (radiation, PBL, LSM)**
- **Add ensemble members**
- **Improve data assimilation**

Why focu

• For mar … the
precipit … snow:

CSs

• Yet sno … nt in
terms o … d size
distribu

from Reisner et al. (1998)

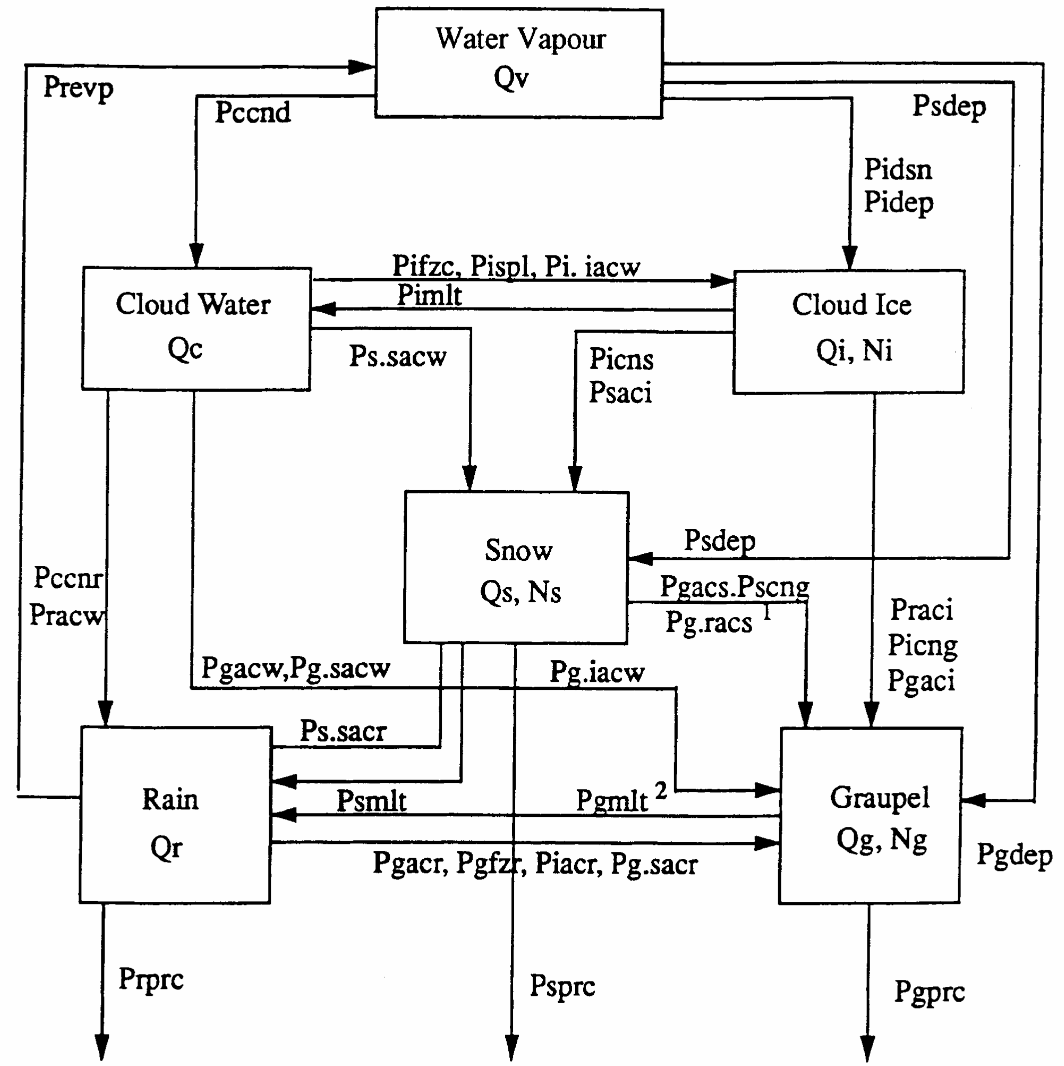

Three aspects of the representation of snow in bulk schemes:

1. **Size distribution**
2. **Shape and density assumptions (i.e., mass-diameter relationship)**
3. **Velocity-diameter relationship**

A case will be made for:

1. **Choosing a reasonable/relevant habit**
2. **Enforcing "habit consistency" throughout the scheme**
3. **Diagnosing (as in Meyers et al. 1997) or predicting habit variability**

1. Size distribution

$$\hat{N}_s(D) = N_{0s} \exp(-\lambda_s D)$$

Integrating the third moment over all sizes yields

$$\rho_{\mathrm{air}} q_s = \frac{\pi N_{0s} \rho_{\mathrm{snow}}}{\lambda_s^{\ 4}} = f(N_{0s}, \lambda_s)$$

q_s is predicted;
specify N_{0s}, and solve for λ_s;
or alternatively, specify λ_s, and solve for N_{0s}.

Intercept and slope parameters measured by aircraft particle imagers throughout IMPROVE-1 and IMPROVE-2, as a function of temperature

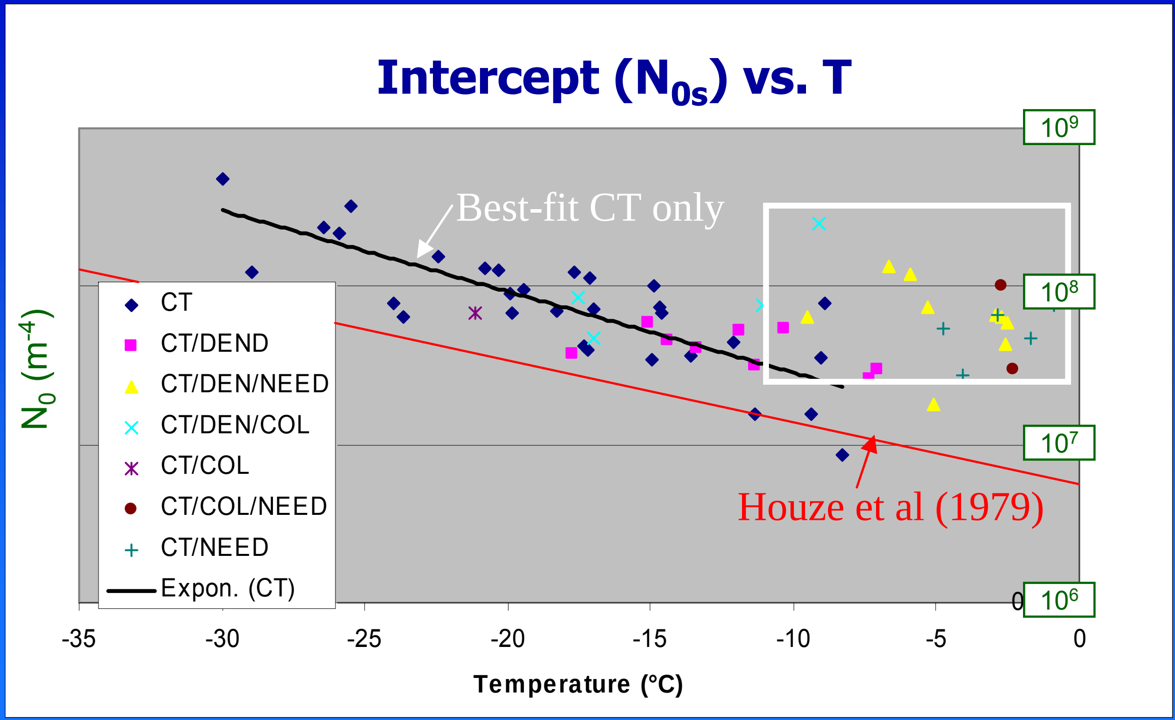

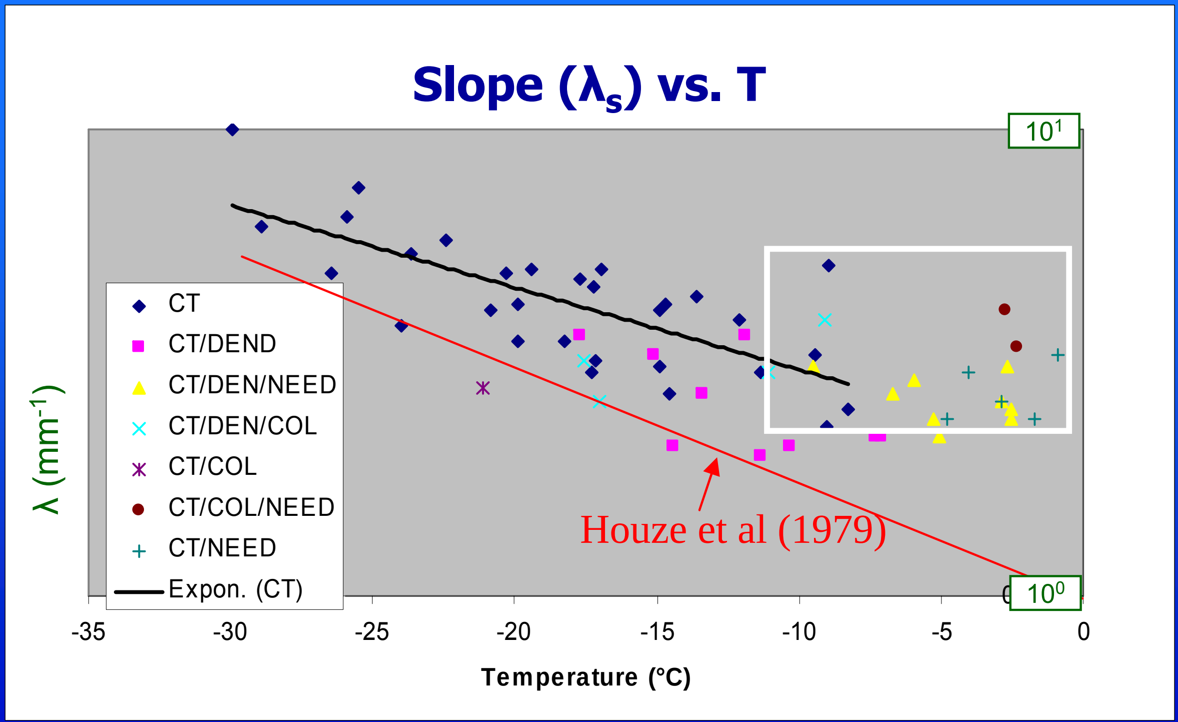

2. Snow particle shape and density

Many bulk schemes (R-T, Tao and Simpson 1993, Ferrier 1994) assume snow particles are <u>spheres</u> of <u>constant density</u>, implying a mass-diameter relationship of:

$$m(D) = \rho_{\mathrm{snow}}(\pi/6)D^3$$

However, observational and theoretical studies yield more general, habit-dependent power-law relationships of the form

$$m(D) = a_m D^{b_m} \;,$$

which can also be implemented in bulk schemes (Cox 1988, Meyers et al. 1997).

Constants in the *m-D* power law relationships for various crystal aggregate types (from Locatelli and Hobbs 1974), and for model snow spheres

Habit	a_m (mg mm^{-bm})	b_m
Dendrites	0.0141	2.19
Cold-type	0.0370	1.90
Needles	0.0092	2.01
Model spheres	0.0520	3.00

General expression for relationship between q_s, N_{0s}, and λ_s:

$$\rho_{\text{air}} q_s = \frac{a_m N_{0s} \Gamma(b_m + 1)}{\lambda_s^{\,b_m + 1}}$$

Variation of spectral slope with particle habit (for fixed values of N_{0s} and q_s)

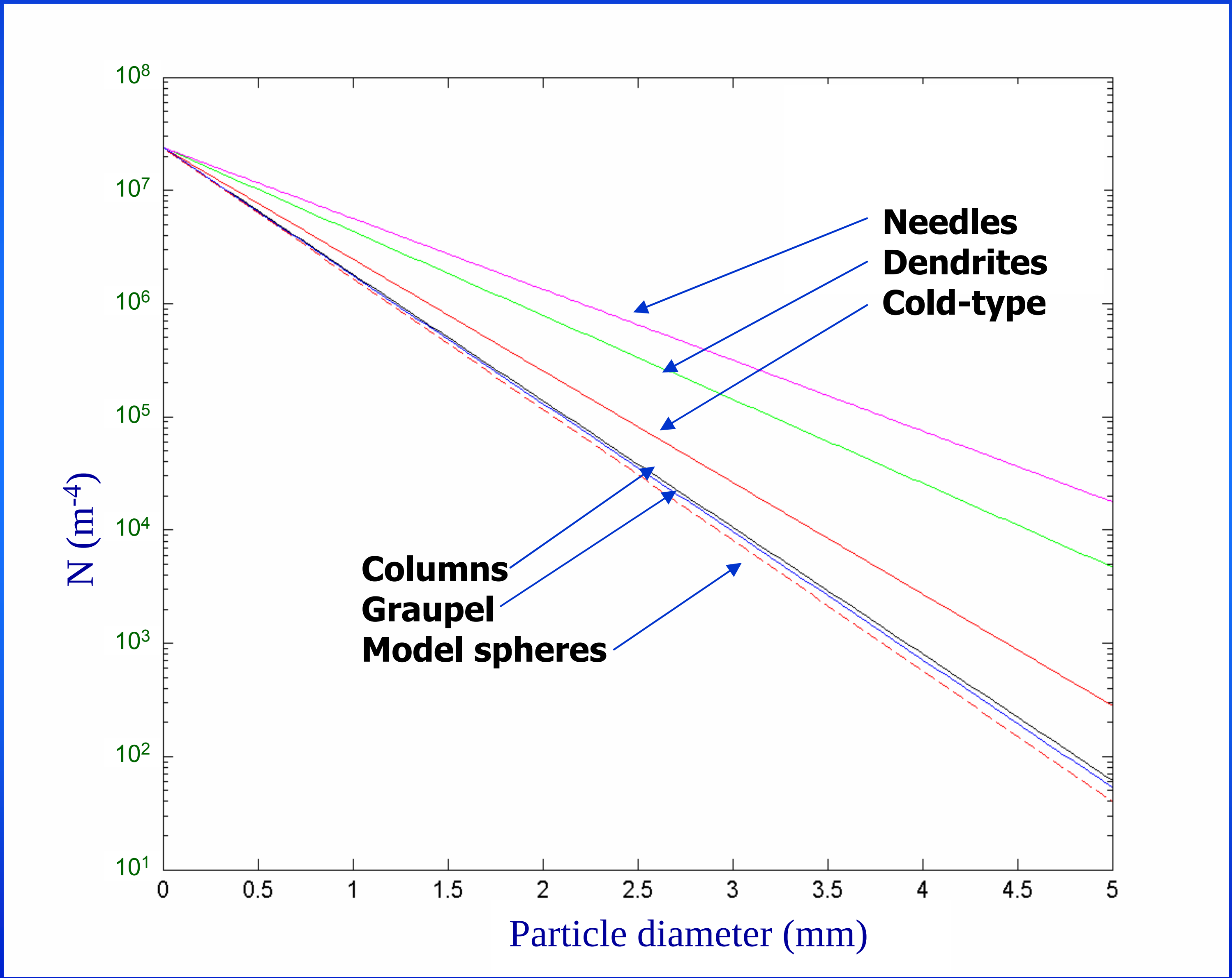

3. Snow fall speed

Observational and theoretical studies provide habit-dependent power-law relationship between the terminal fall speed of a particle and its diameter (a *V-D* relationship) of the form

$$V(D) = a_v D^{b_v} \quad ,$$

Combining with the exponential size distribution and the appropriate *m-D* relationship (for the same particle habit) and integrating, one obtains the *mass-weighted* terminal fall speed for snow particles <u>of that habit</u>:

$$\bar{V} = \frac{a_{\mathrm{v}}\,\Gamma\left(b_{\mathrm{m}} + b_{\mathrm{v}} + 1\right)}{\lambda_s^{\,b_{\mathrm{v}}}\,\Gamma\left(b_{\mathrm{m}} + 1\right)}$$

Mass-weighted terminal fallspeed for various particle habits and snow mixing ratios

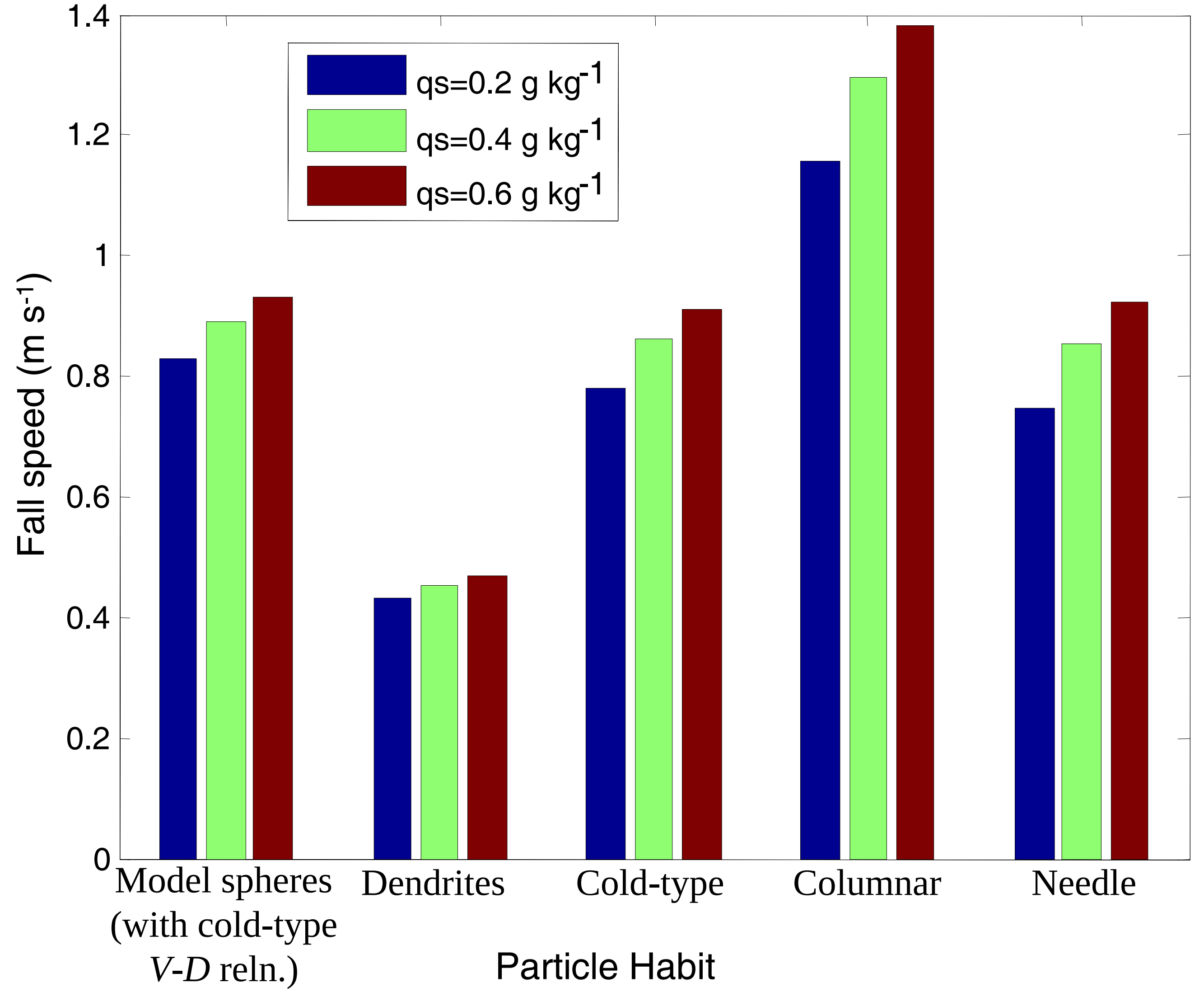

Example: Frontal rainband observed off the Washington coast during IMPROVE-1 (1-2 February 2001)

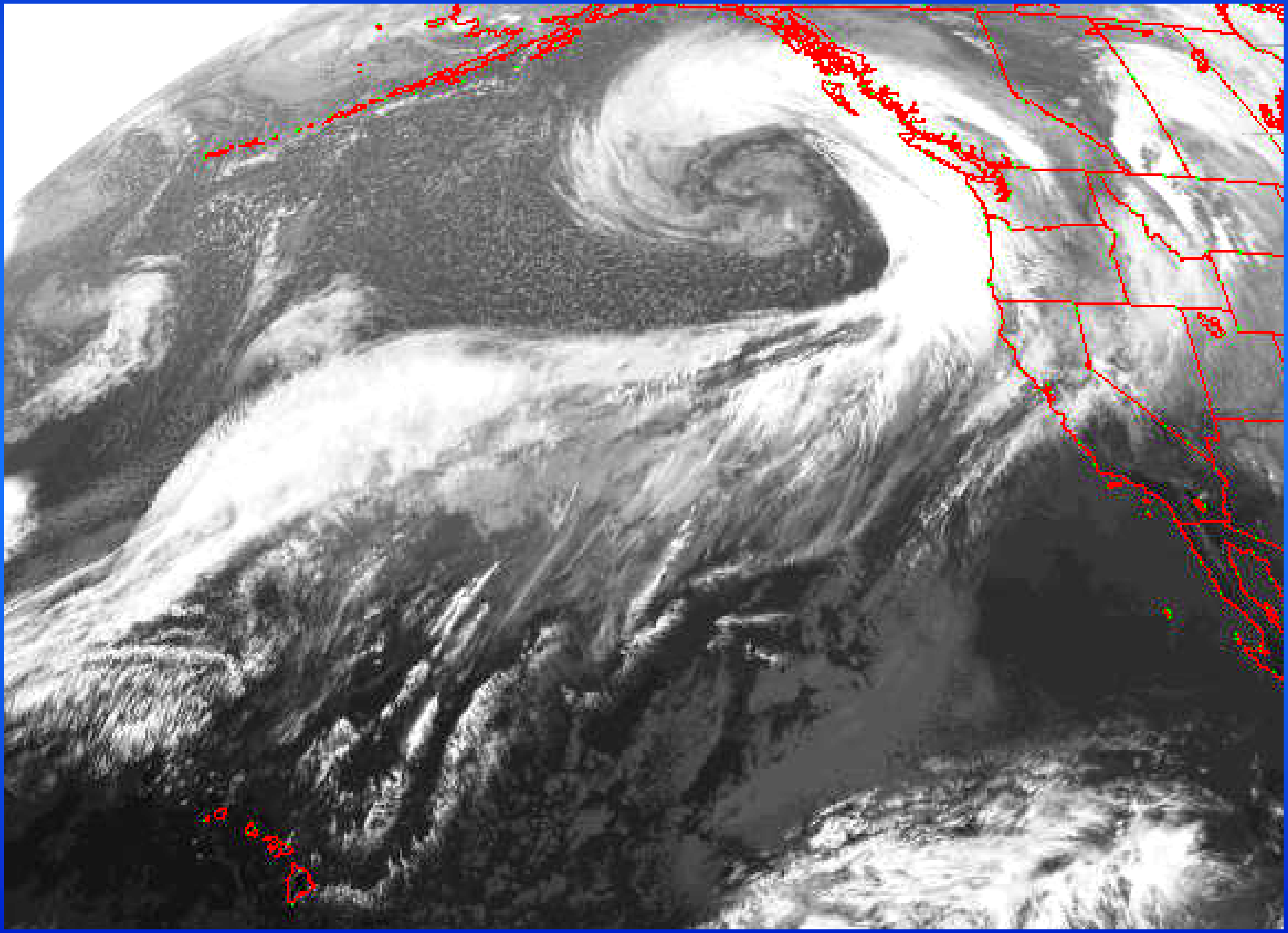

14-h MM5 forecast of 1-h precip, 12-km grid, R-T microphysics

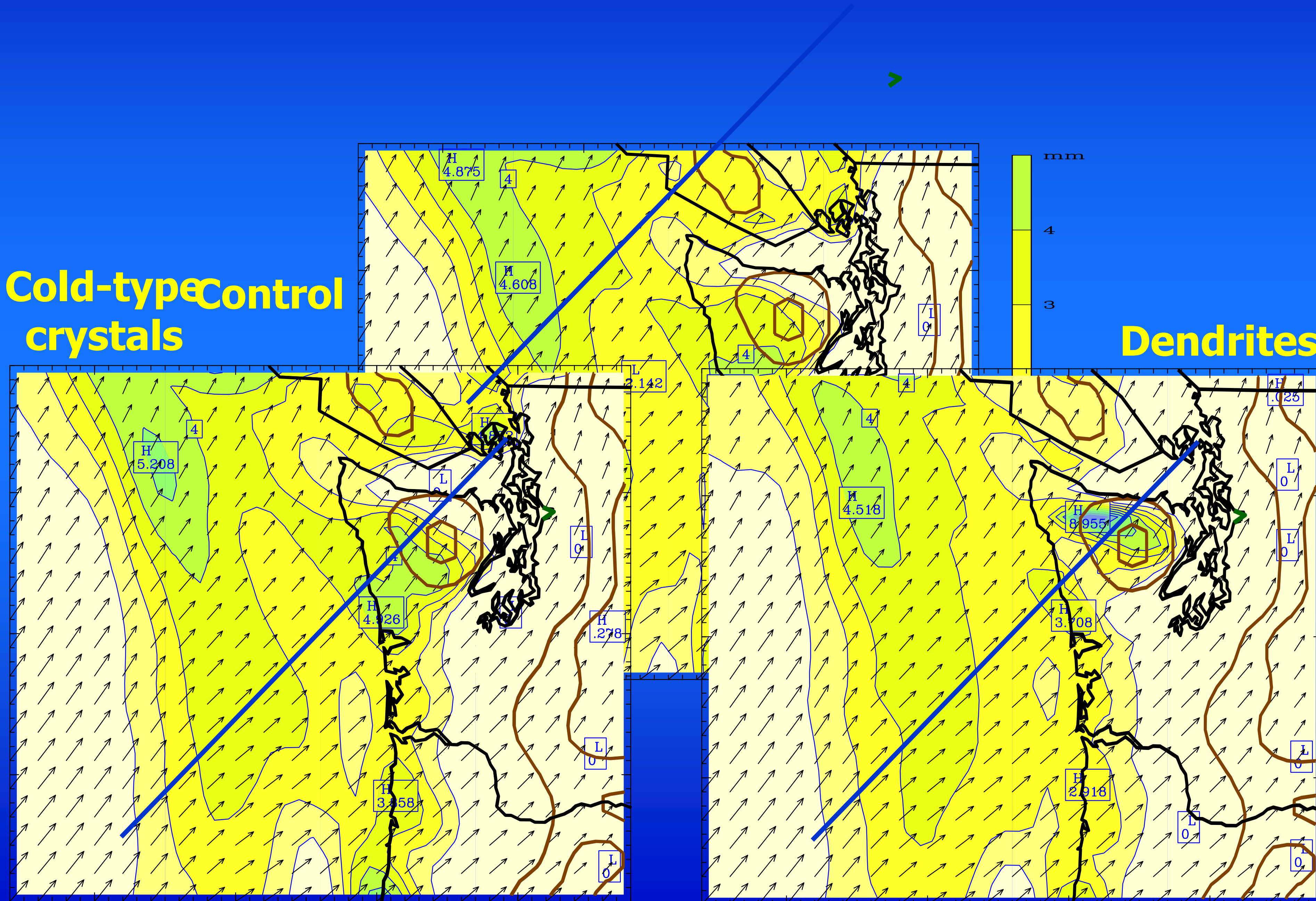

Control

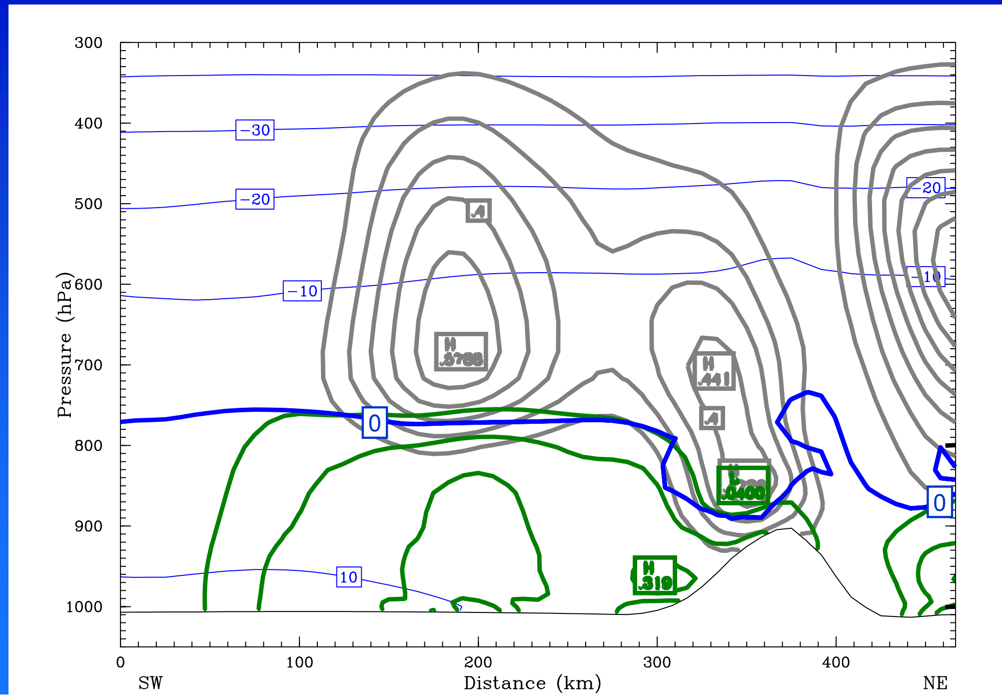

Contours:

q_{snow} (g kg^{-1})

q_{rain} (g kg^{-1})

T (°C)

Cold-type crystals

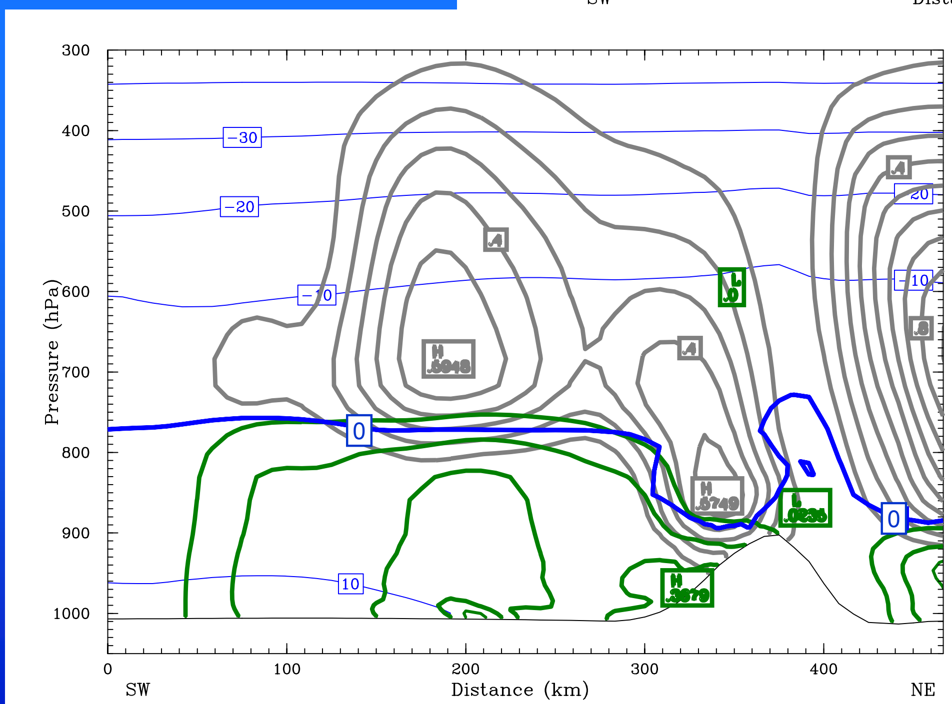

Dendrites

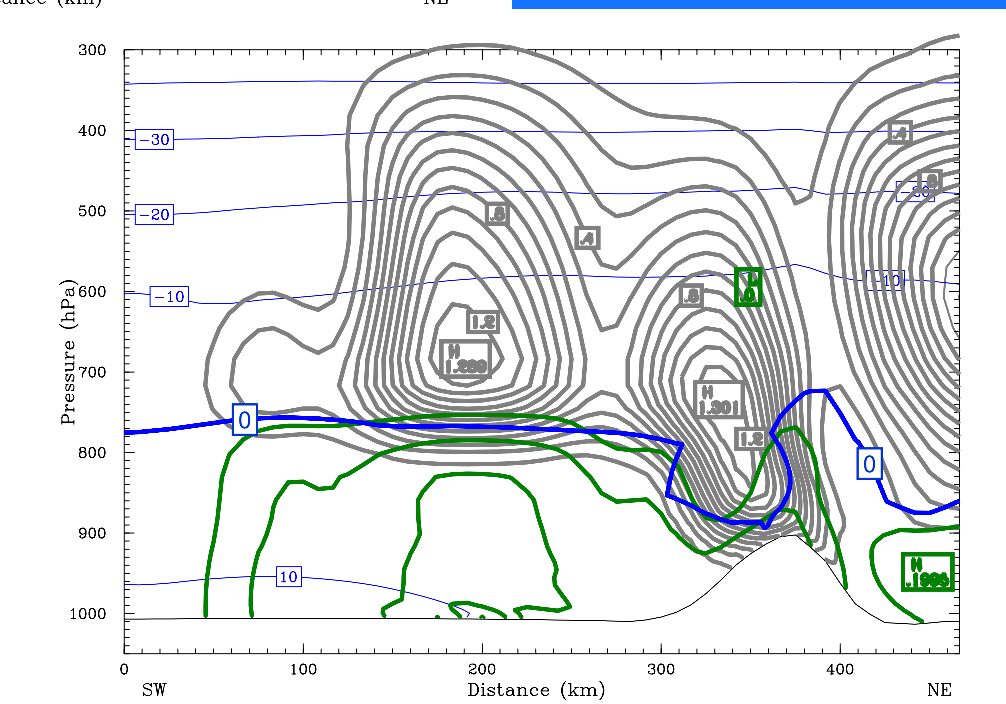

Contours:
precip rate ($mm\ h^{-1}$)
T (°C)

Control

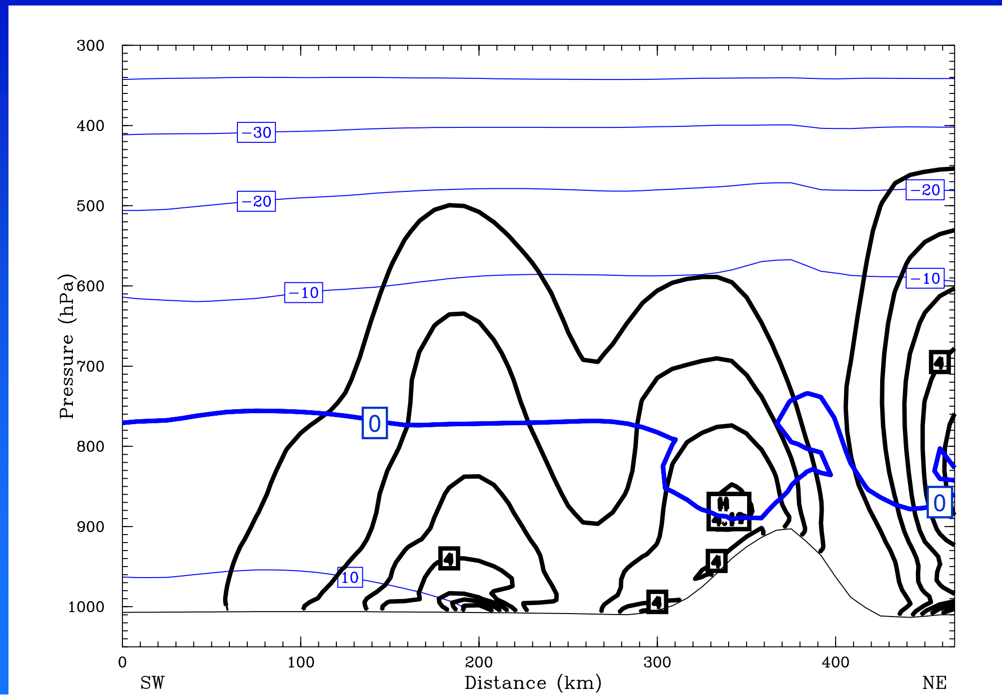

Cold-type crystals

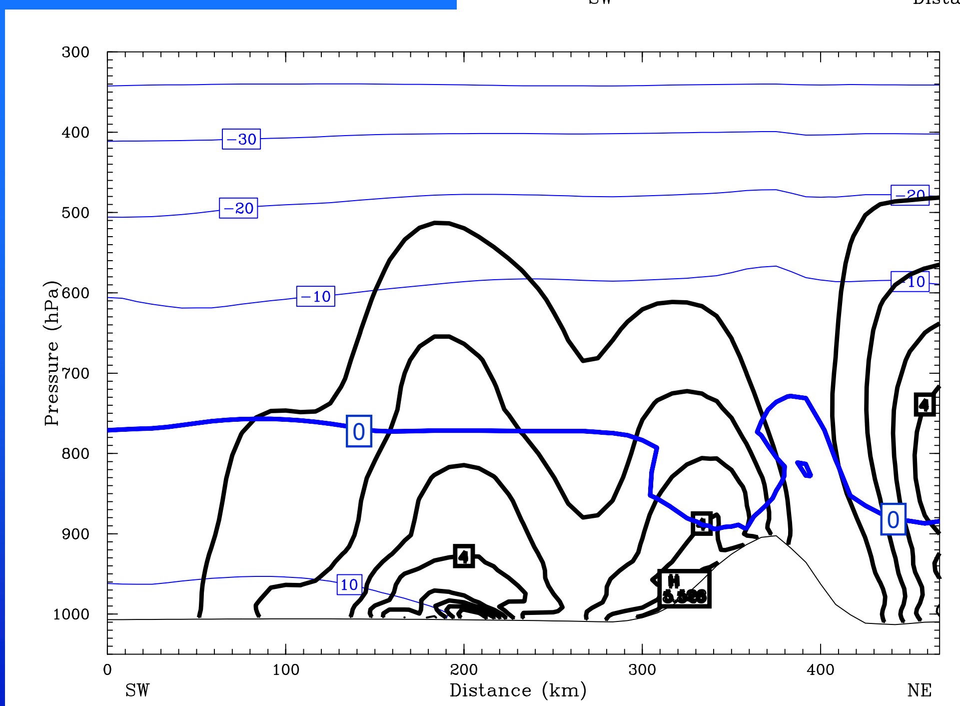

Dendrites

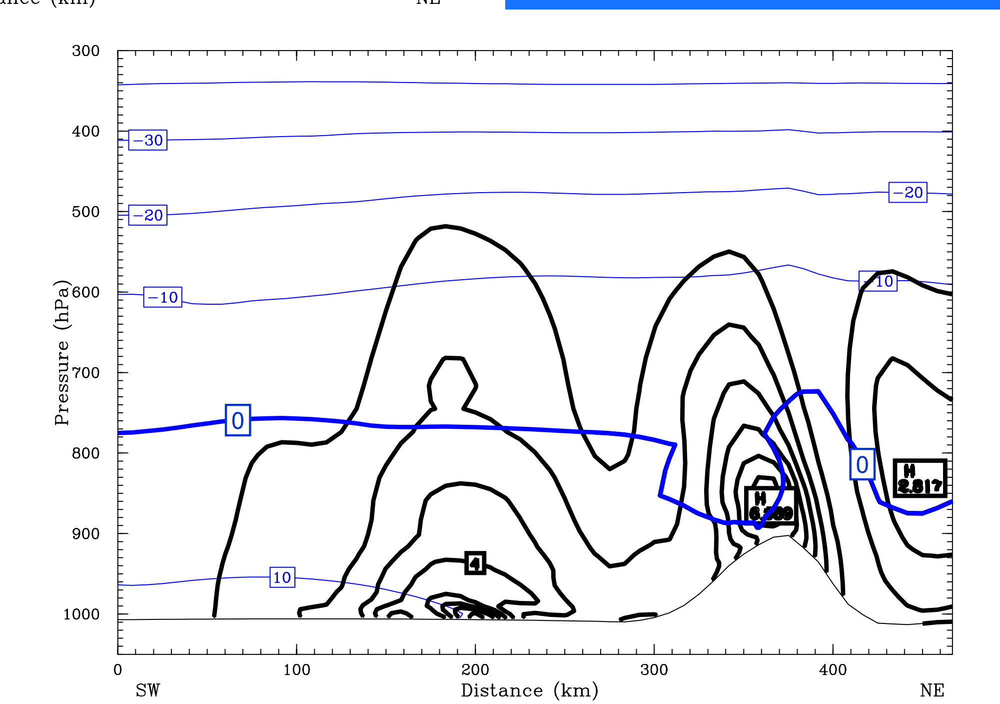

Recommendations / Future Work:

1. Constant density spheres are not a good representation of most snow particle types.
2. Enforce "habit consistency" for the various habit-dependent aspects of the scheme (size distribution, *m-D* and *V-D* relationships, capacitance for depositional growth, etc.)
3. Examine ways to skew the distribution toward smaller particles when ice enhancement is active. Can this be done without going to a double-moment scheme?
4. Implement particle habit diagnosis (Meyers et al. 1997)
5. Develop habit *prognosis*, to test the effectiveness of the simpler habit *diagnosis*.

Global ice particle spectra, Ryan (1996)

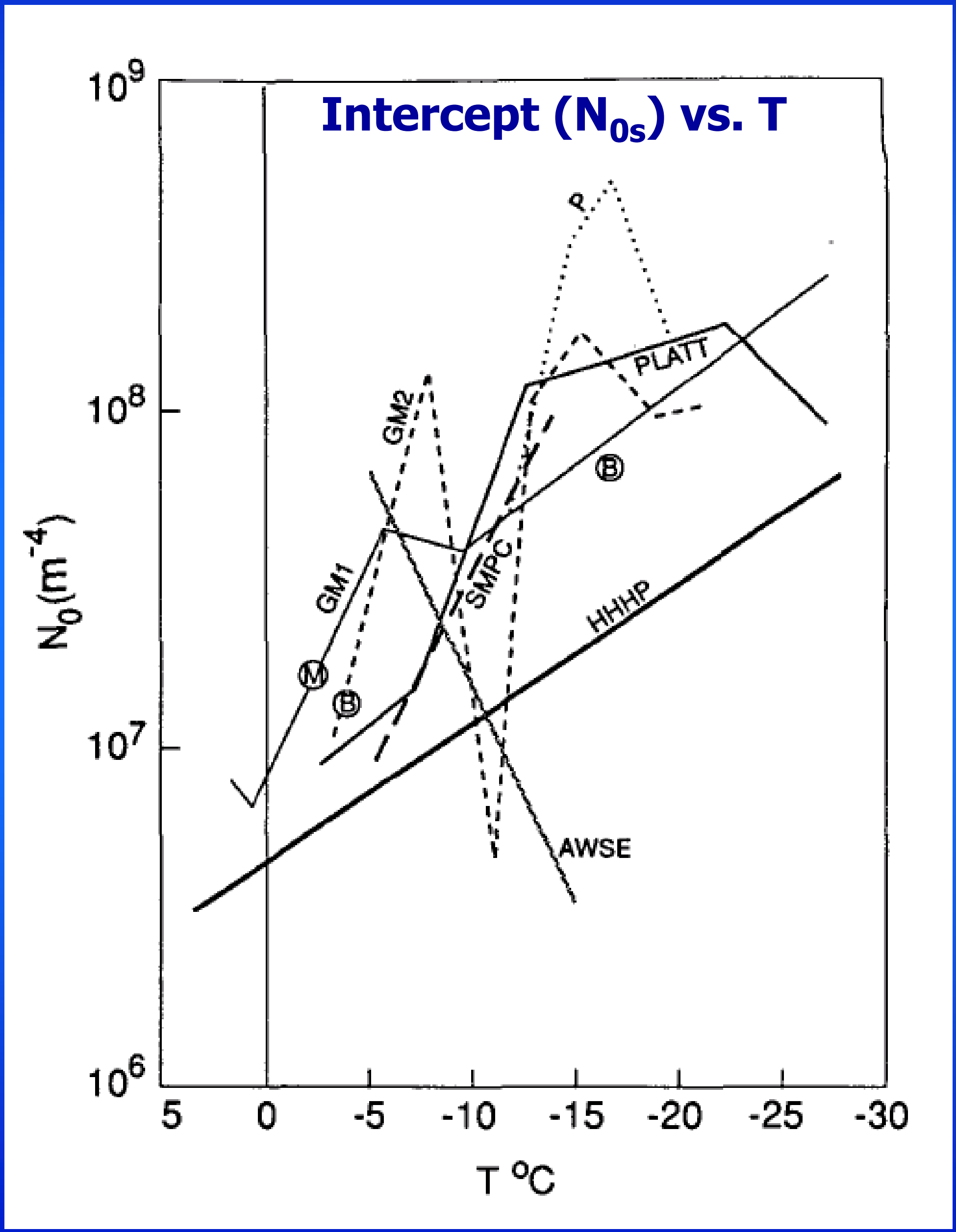

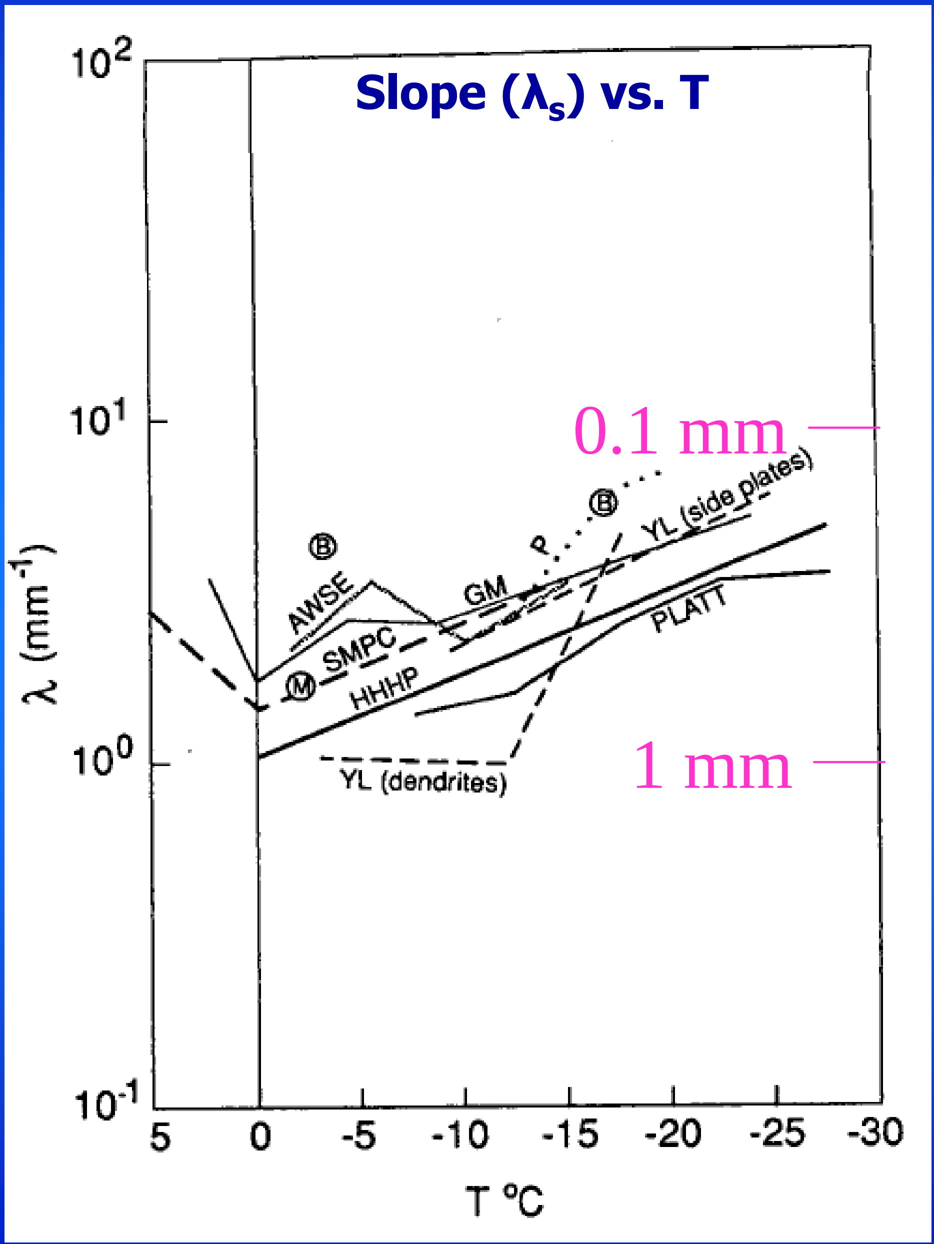

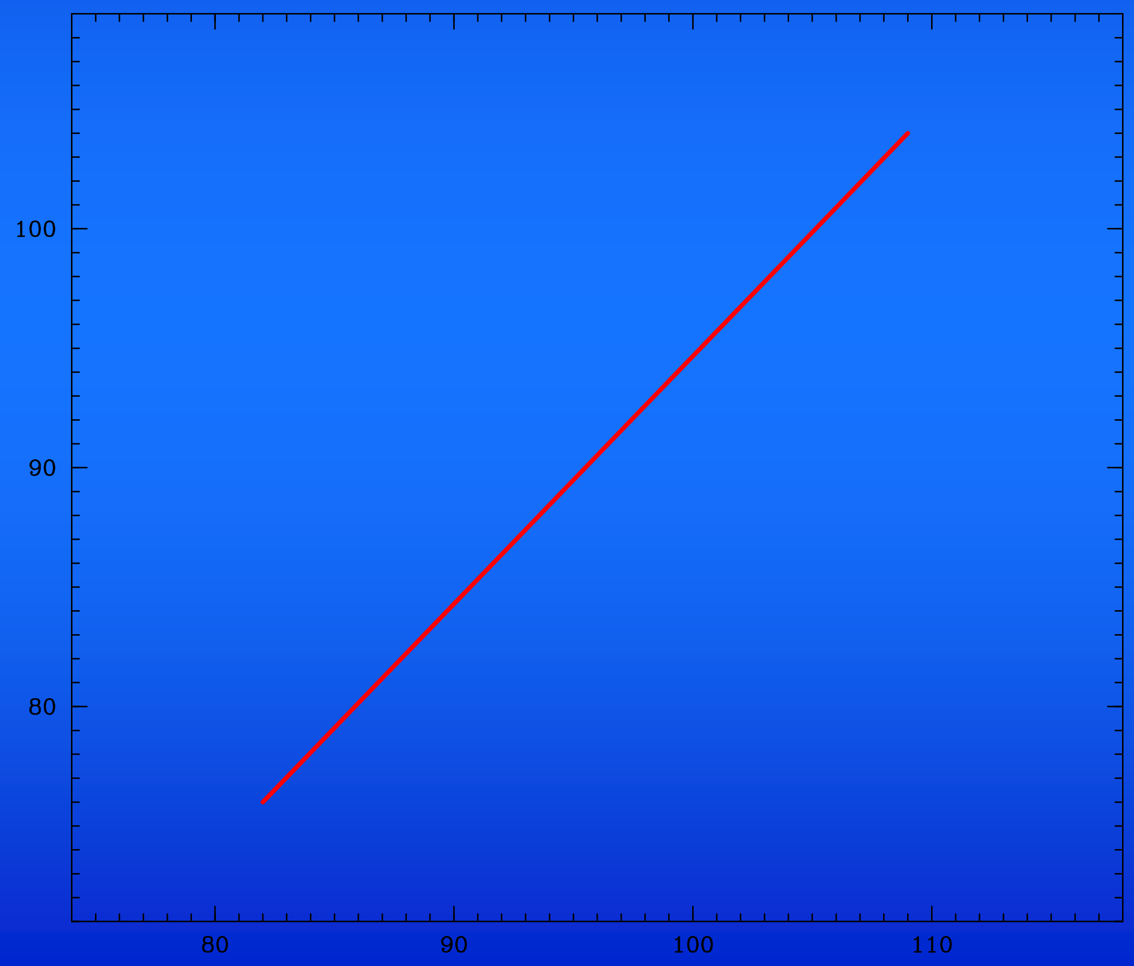

100
90
80
80
90
100
110

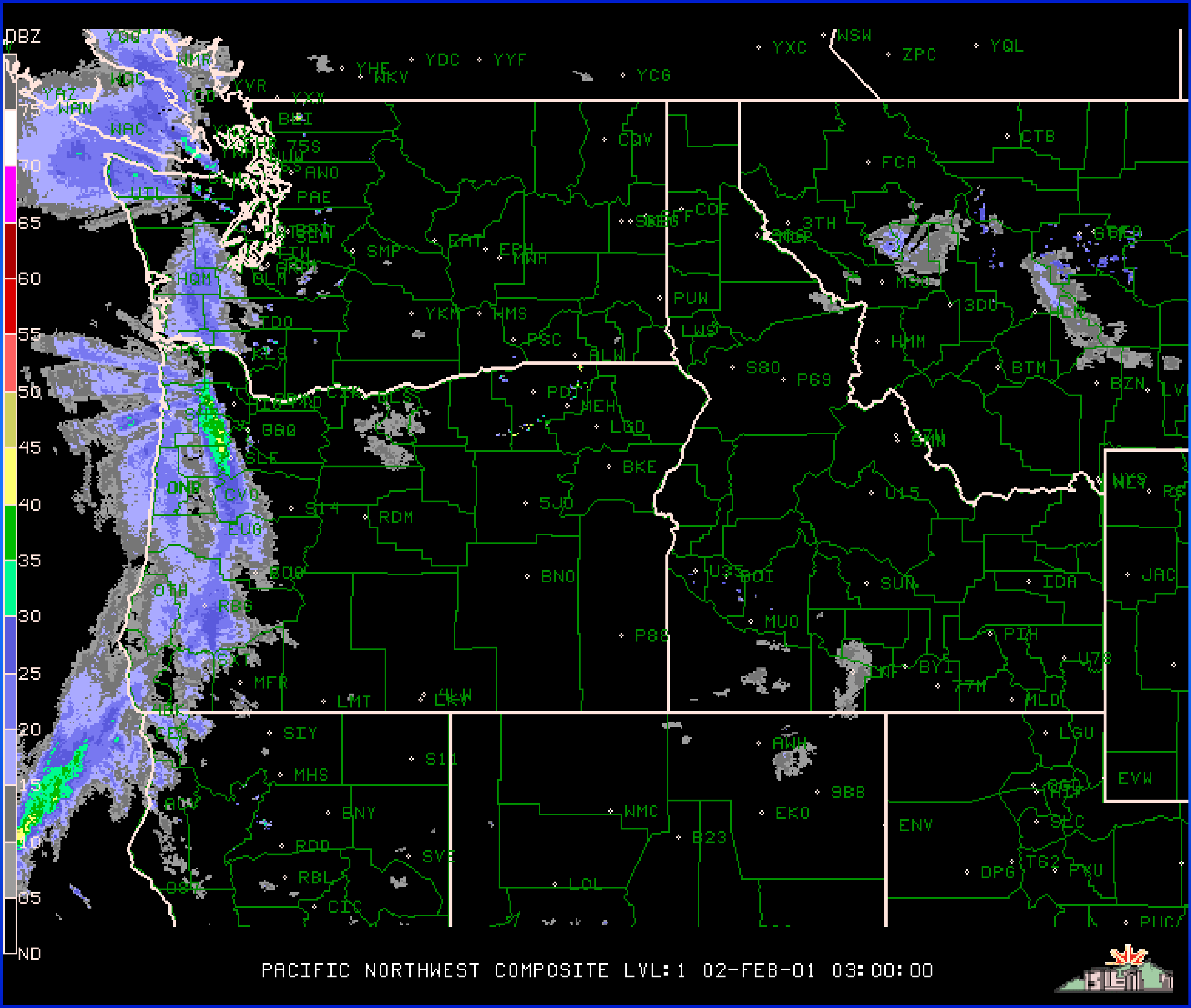
DBZ
75
70
65
60
55
50
45
40
35
30
25
20
15
10
05
ND
PACIFIC NORTHWEST COMPOSITE LVL:1 02-FEB-01 03:00:00

Papers submitted for a special "IMPROVE" issue of the *Journal of the Atmospheric Sciences:*

Bond, N. A., B. F. Smull, M. T. Stoelinga, C. P. Woods, A. Haase, and J. D. Locatelli, "The Evolution of a Cold Front over Quasi-2D Terrain: Coordinated Aircraft Observations of the 8-9 December 2001 Wide Cold Frontal Rainband during IMPROVE-2"

Colle, B. A., M. F. Garvert, J. B. Wolfe, and C. F. Mass, "Microphysical Budgets and Sensitivity Studies for the 13-14 December 2001 IMPROVE-2 Event"

Evans, A. G., J. D. Locatelli, M. T. Stoelinga, and P. V. Hobbs, "The IMPROVE-1 Storm of February 1-2, 2001. Part II: Cloud Structures and the Growth of Precipitation"

Garvert, M. F., B. A. Colle, and C. F. Mass, "Synoptic and Mesoscale Evolution of the 13-14 December 2001 IMPROVE II Storm System and Comparison with a Mesoscale Model Simulation"

Garvert, M. F., C. P. Woods, B. A. Colle, C. F. Mass, P. V. Hobbs and J. B. Wolfe, "Comparisons of MM5 Model Simulations of Clouds and Precipitation with Observations for the 13-14 December 2001 IMPROVE-2 Event"

Houze, R. A., and S. Medina, "Turbulence as a Mechanism for Orographic Precipitation Enhancement"

Medina, S., B. F. Smull, and R. A. Houze, "Airflow Patterns in Orographic Precipitation Events over the European Alps and the Oregon Cascades"

Ikeda, K, E. A. Brandes, and R. M. Rasmussen, "Polarimetric Radar Observation of Multiple Freezing Levels"

Locatelli, J. D., M. T. Stoelinga, M. F. Garvert, and P. V. Hobbs, "The IMPROVE-1 Storm of February 1-2, 2001. Part I: Development of a Forward-Tilted Cold Front and a Warm Occlusion"

Woods, C. P., M. T. Stoelinga, J. D. Locatelli, and P. V. Hobbs, "Cloud Structures, Microphysical Processes and Synergistic Interaction between Frontal and Orographic Forcing of Precipitation during the December 13, 2001 IMPROVE-2 Event over the Oregon Cascades"

Yuter, S. E., D. Kingsmill, L. B. Nance, and M. Löffler-Mang, "Observations of precipitation characteristics near and within the melting layer"

Outline:

- Microphysical issues (as represented in the MM5's mixed phase scheme), from observations and modeling of IMPROVE case studies
- Hypotheses for important interactions between mesoscale processes and microphysics
- "Studies of opportunity": interesting features elucidated by the IMPROVE data set

Evidence of excessive supersaturation with respect to ice in deep frontal clouds (Locatelli et al. 2004)

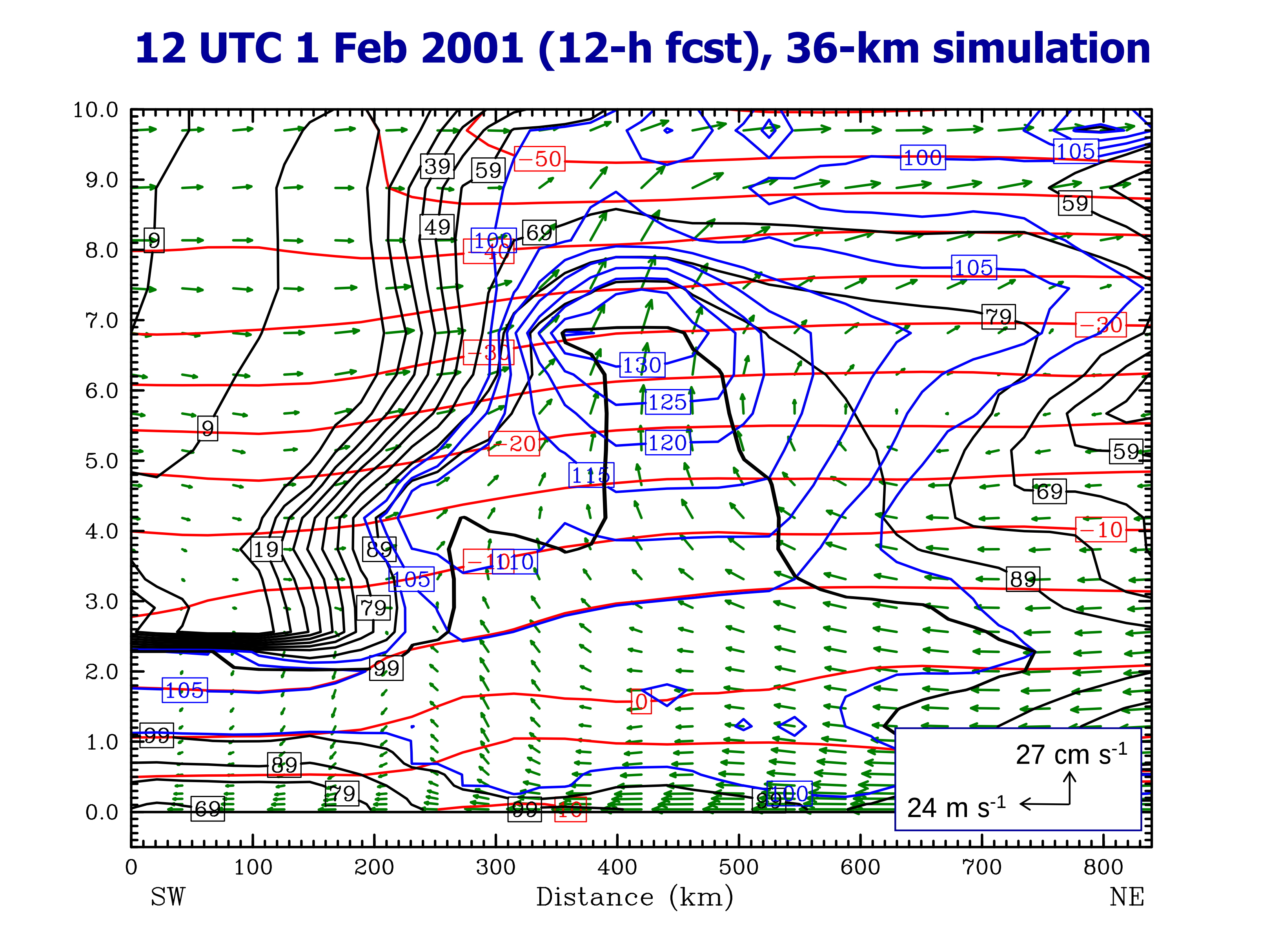

Evidence of excessive supersaturation with respect to ice in deep frontal clouds

00 UTC 2 Feb 2001 (24-h fcst), 36-km simulation

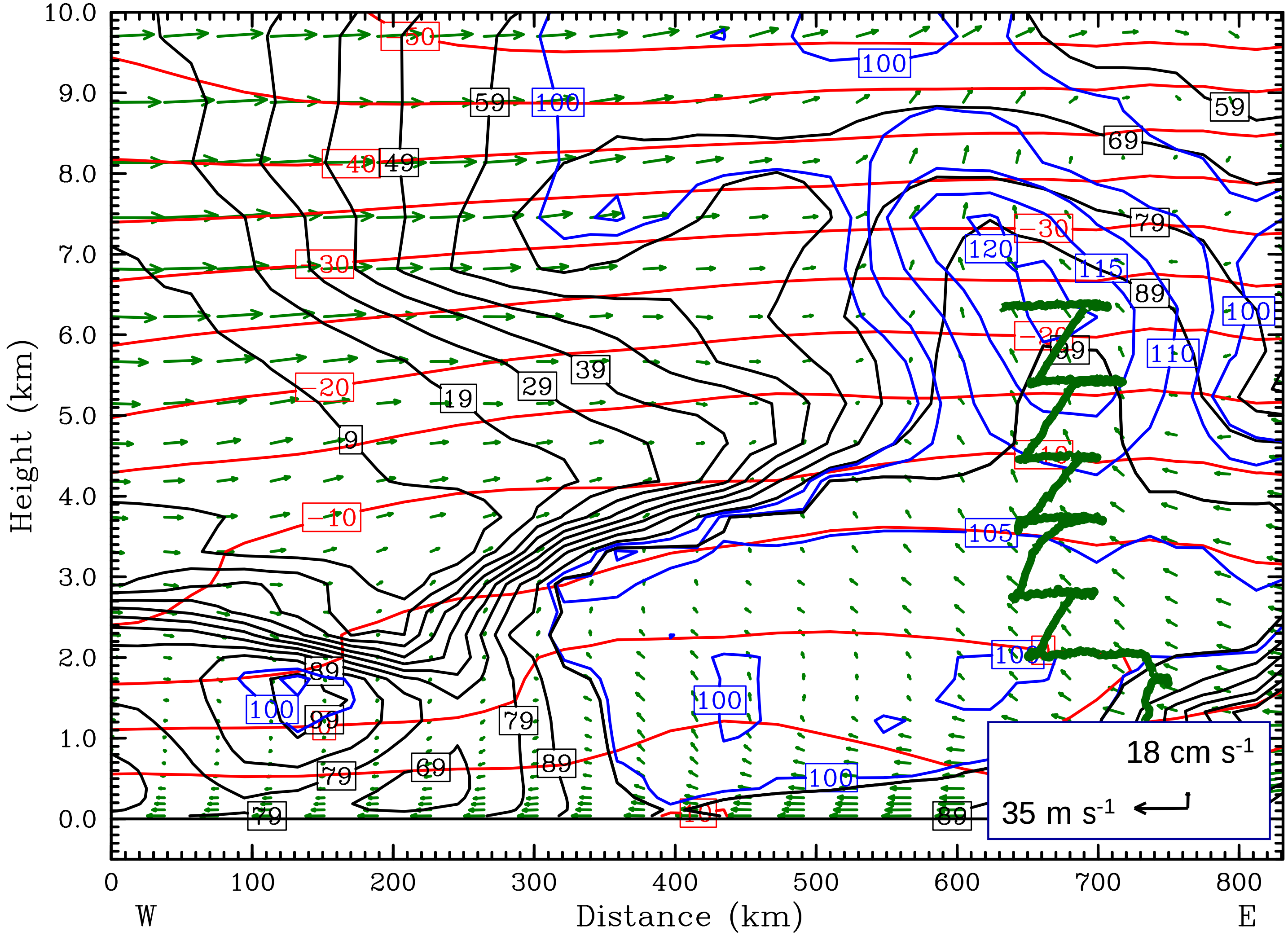

Summary of observations from Convair-580 flight stack:

In regions where model indicated high ice supersaturation:

- measured RH was generally near ice saturation
- Negligible liquid water was detected
- Ice crystal habits were generally found to be sub-water-saturated types, or inconclusive (notably, no dendrites in the dendritic growth zone)

One possible problem with the Rutledge and Hobbs (1983) formulation for growth of snow by deposition (PSDEP):

Although the RH83 equation uses capacitance for a 2-D plate, it assumes the population is comprised of spherical particles.

For a given supersaturation, the mass of a growing particle as a function of time behaves as follows:

- 3-D growth (e.g., spherical particle): $m(t) \propto \dfrac{t^{3/2}}{\rho_s^{1/2}}$
- 2-D growth (e.g., plate, dendrite): $m(t) \propto \dfrac{t^{2}}{\rho_s}$
- 1-D growth (e.g., needle): $m(t) \propto \exp\left(\dfrac{\mathrm{const} \times t}{\rho_s}\right)^{1/2}$

(Young 1993)

Growth of snow by deposition is also sensitive to the assumed snow particle size distribution parameters (Garvert et al. 2004)

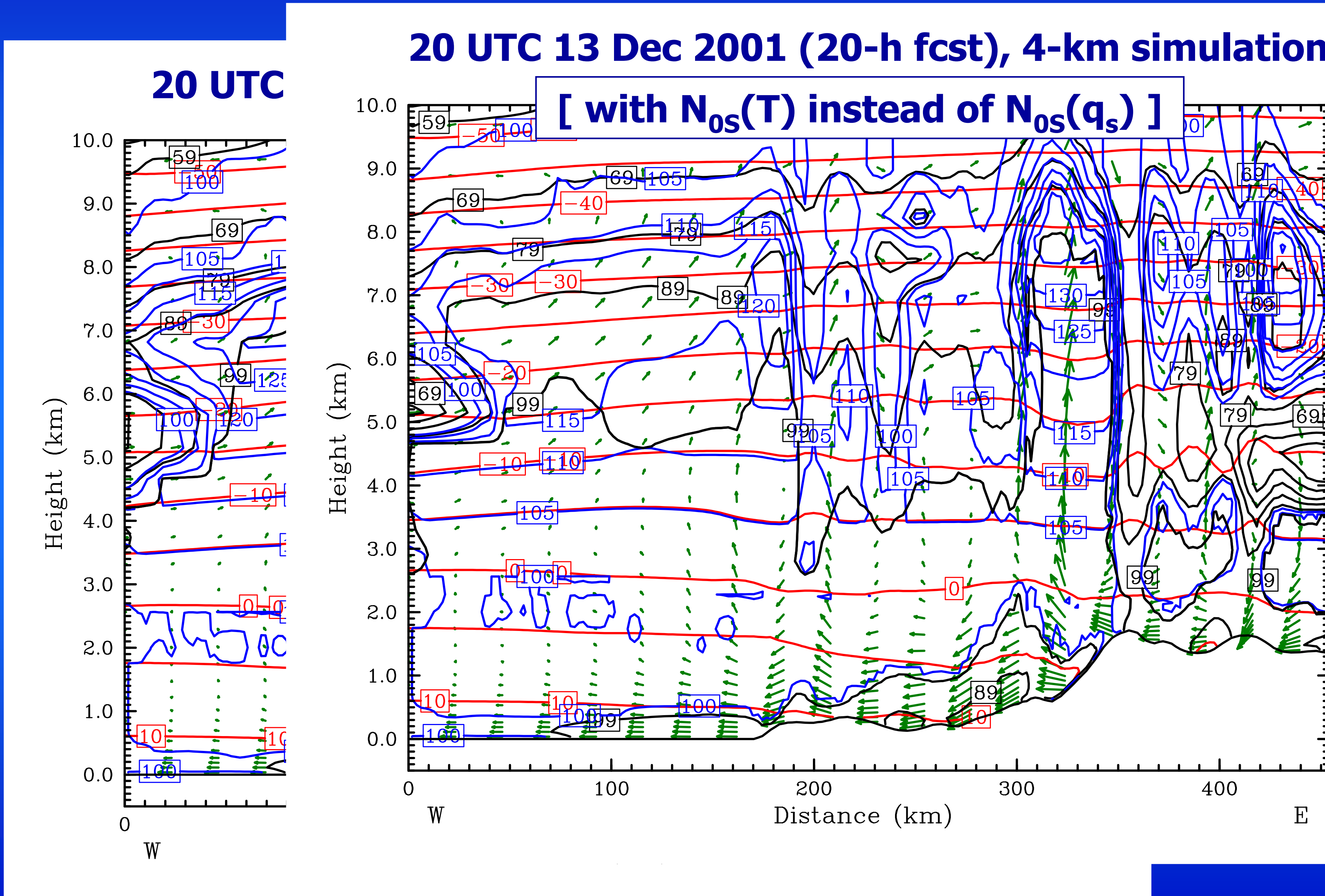

Neither formulation for N_{0S} agrees with the "upside-down" behavior of N_{0S} that was observed in Convair-580 flight tracks during the 13-14 Dec 2001 case. (model spectra from 1.3-km MM5 simulation)

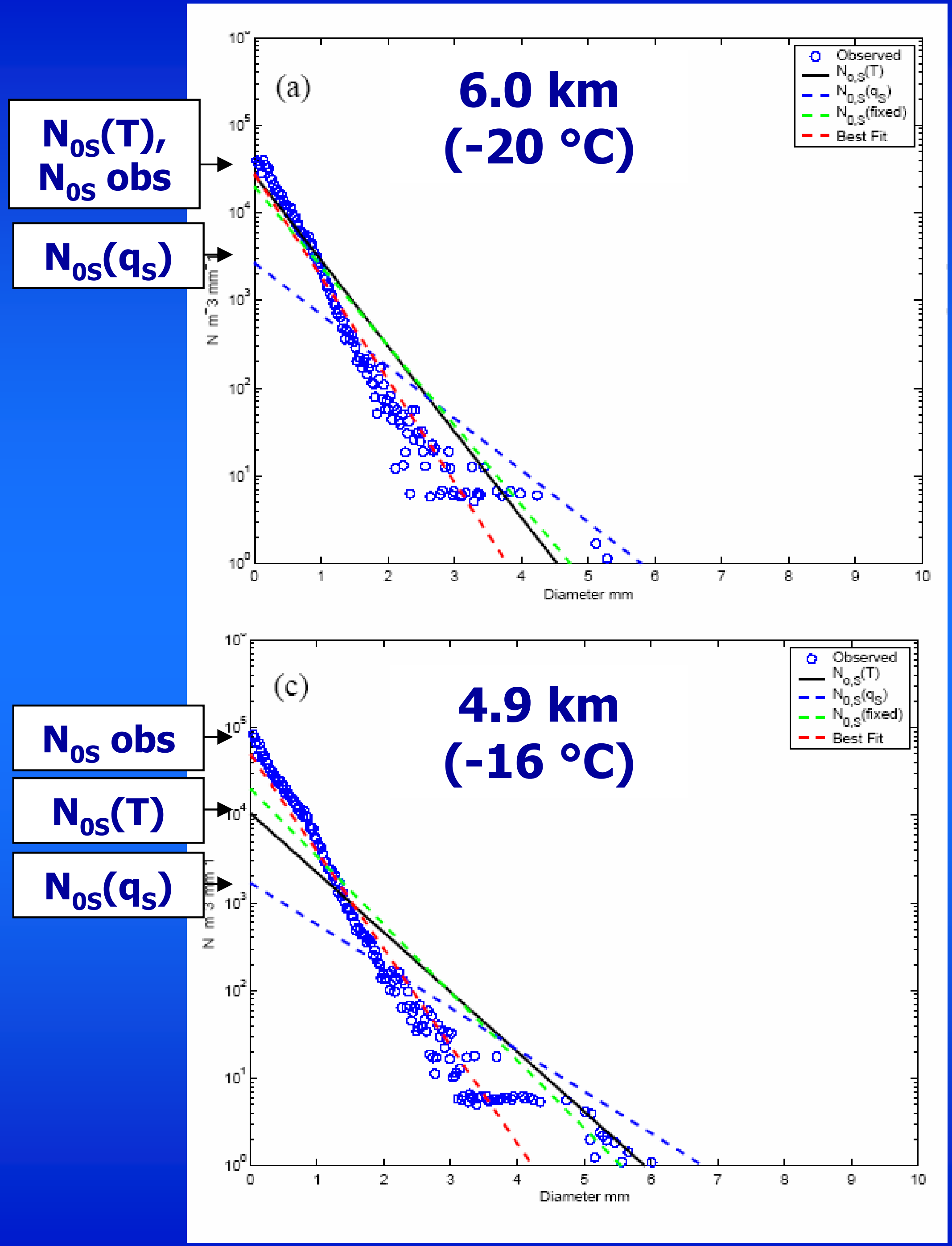

Storm total precipitation verification from the 1.3-km MM5 simulation (Garvert et al. 2004)

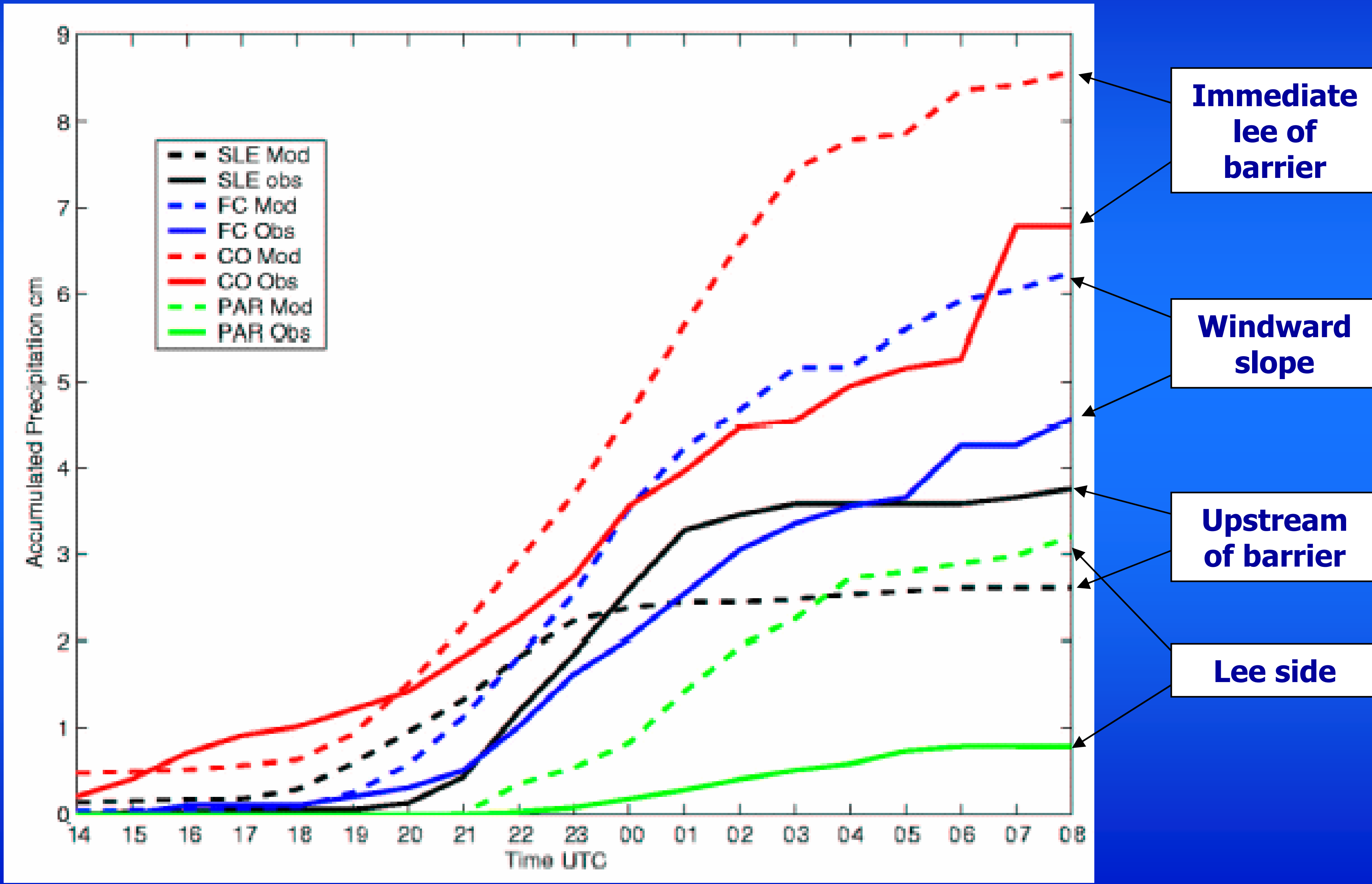

Water mass transfer budget of bulk microphysical scheme for simulation of 13-14 Dec 2001 case (Colle et al. 2004)

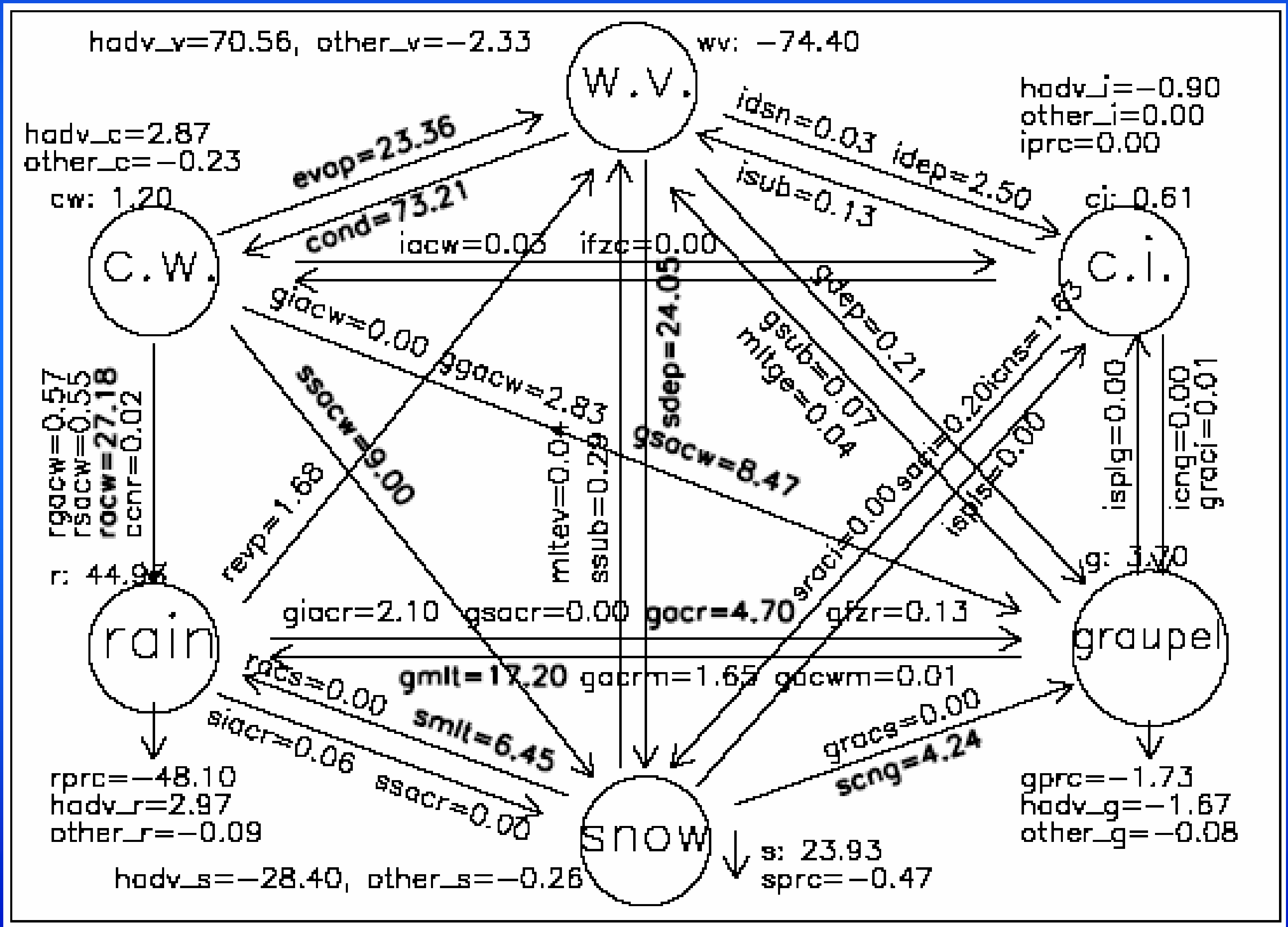

Turbulence as a Mechanism for Orographic Precipitation Enhancement (Houze and Medina 2004)

Hypotheses for important interactions between

Vertically pointing *S*-band (precipitation) radar in the upslope zone

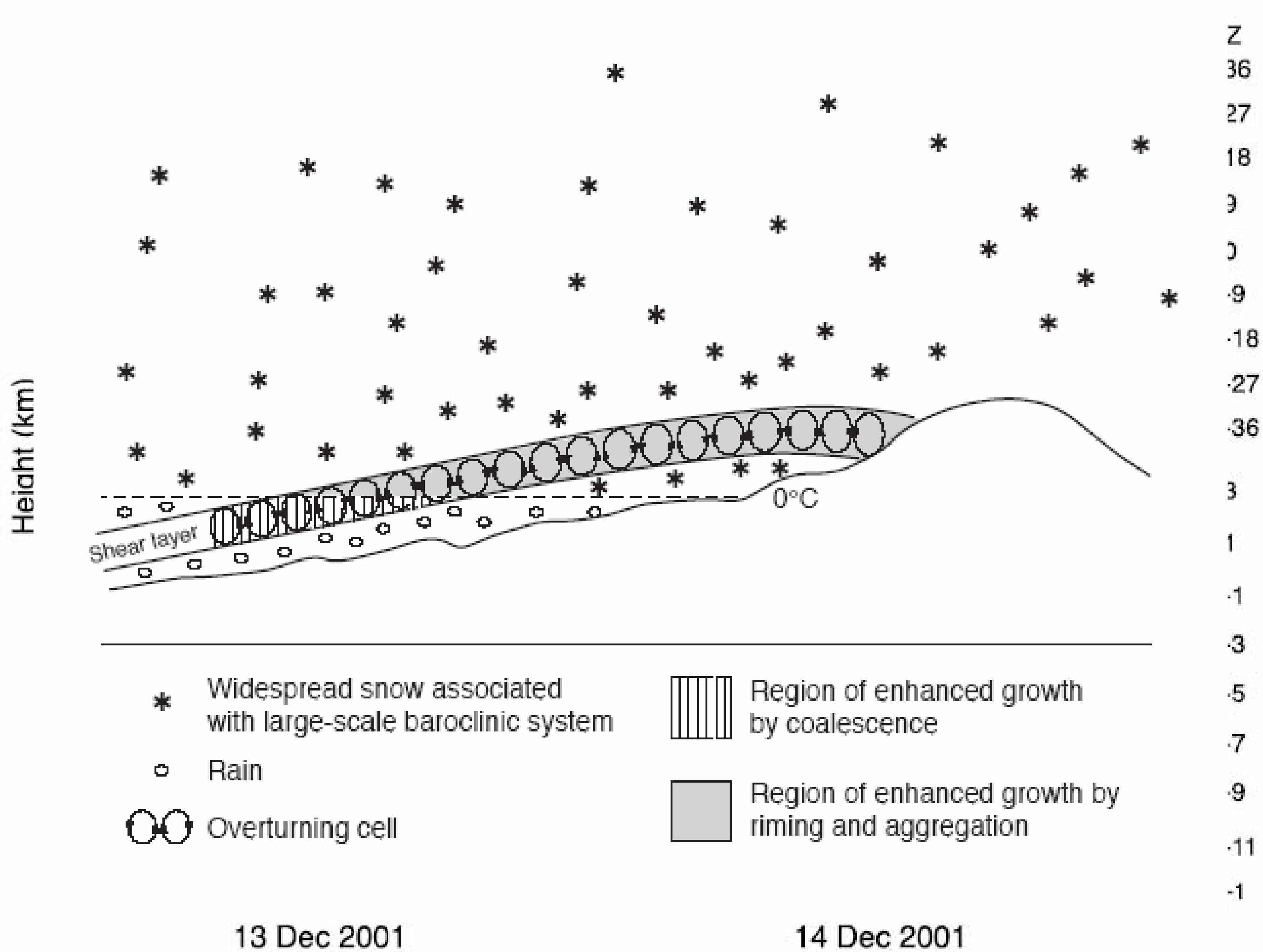

Importance of frontal structure and prefrontal flow for maximizing interaction between frontal and orographic precipitation (Woods et al. 2004)

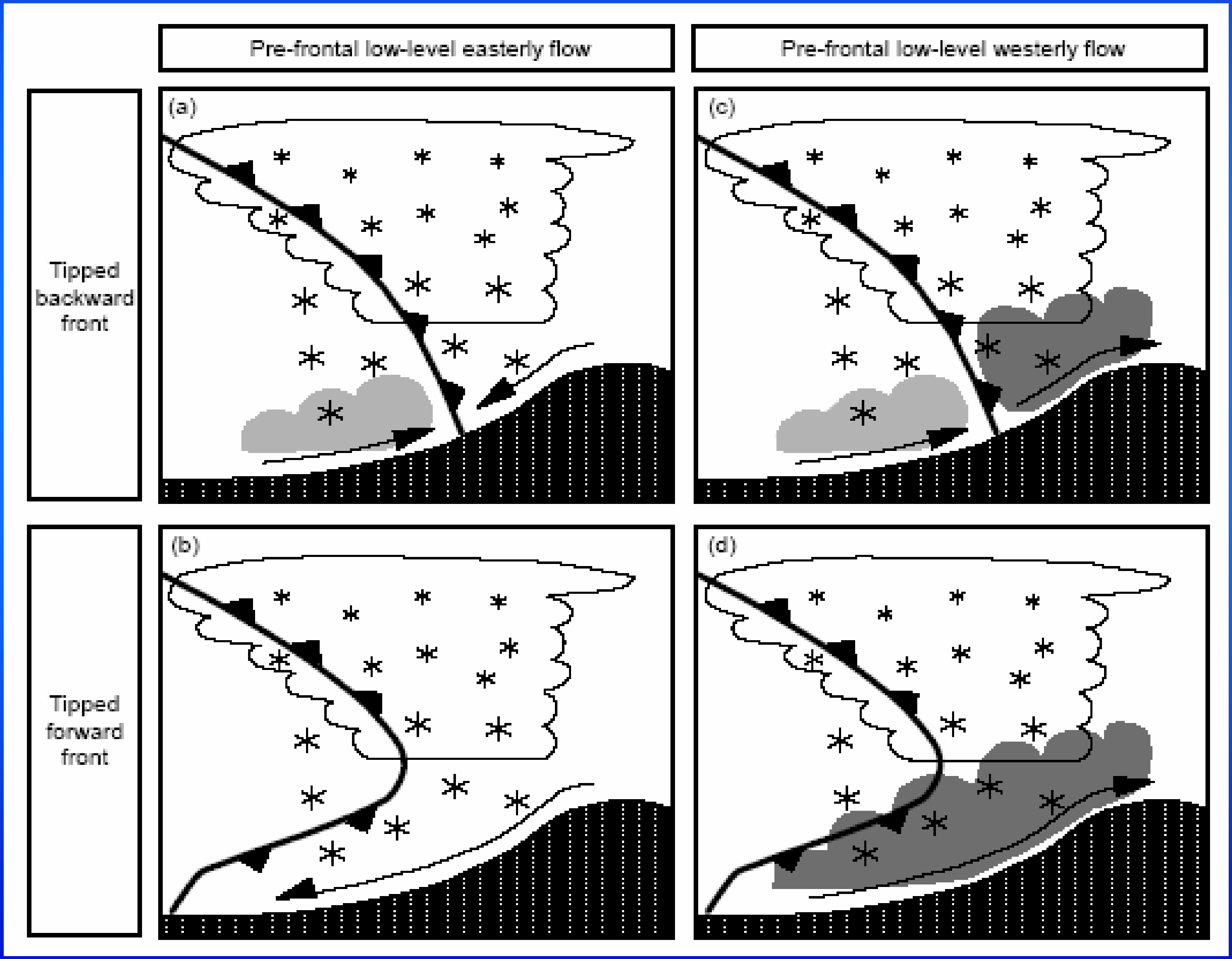

Double brightband within warm-frontal inversion zone (Ikeda et al. 2004)

Unique frontal precipitation phenomena elucidated by the ground-based dual-polarized Doppler (S-Pol) radar